Polymer 50 (2009) 2220–2227

Contents lists available at ScienceDirect

Polymer

journal homepage: www.elsevier.com/locate/polymer

Aliphatic–aromatic copolyesters containing phosphorous cyclic bulky groups

Tachita Vlad-Bubulac*, Corneliu Hamciuc

Institute of Macromolecular Chemistry "Petru Poni", Aleea Gr. Ghica Voda 41A, Iasi 700487, Romania

ARTICLE INFO

Article history:
Received 25 September 2008
Received in revised form
11 March 2009
Accepted 11 March 2009
Available online 19 March 2009

Keywords:
Phosphorus-containing polyesters
Thermotropic liquid crystalline polymers
Thermal stability

ABSTRACT

A series of phosphorus-containing copolyesters was prepared by polycondensation of 2-(6-oxido-6H-dibenz<c,e><1,2>oxaphosphorin-6-yl)-1,4-naphthalene diol, **1**, or of an equimolecular amount of **1** and different aliphatic diols **2**, such as ethylene glycol, 1,3-propanediol, 1,4-butanediol, 1,6-hexanediol and 1,12-dodecanediol, with an aromatic diacid chloride containing two preformed ester groups **3**, namely terephthaloyl-bis-(4-oxybenzoyl-chloride). The copolyesters exhibited good thermal stability having the decomposition temperature above 375 °C. The glass transition temperature was in the range of 96–146 °C. The polymers exhibited thermotropic liquid crystalline behavior, as was observed with polarized optical microscopy. DSC and X-ray experiments were also found in concordance with mesophase formation.

1. Introduction

Polyesters are well known as high performance engineering thermoplastics because of their good thermal stability, chemical resistance and excellent mechanical properties [1]. Main chain thermotropic polyesters presented much interest in the last years because of their many industrial and commercial applications [2]. However, they have the disadvantage of poor melt-processability because they possess high melting and isotropization temperatures [3–6]. The objectives of designing melt processable polyesters with nematic structure are to reduce the melting temperature below the thermal stability limit and to obtain a melt that remains nematic until the onset of decomposition. There are some modification methods to control the phase transition temperatures and to improve the processability, such as the introduction of flexible spacer [7–9], the addition of bulky or nonsymmetrical substituents [10], or the use of nonlinear or bent monomers [11–13]. Another useful approach for reducing the melting temperature of the polymers and increasing the solubility is the copolymerization of monomers by which the symmetry of the structure is lowered and the lateral packing is disrupted [14–16].

Like other organic polymeric materials, the flammability of the polyesters is shortcoming in some applications. An attractive synthetic approach to improve flame retardancy and thermal oxidative stability of the polymers is the incorporation of phosphorus into their unit structure. Phosphorus-containing polymers are able to increase the char during burning, and thus decrease the amount of flammable zone and reduce the heat transfer from the flame to the material. In addition, phosphorus-containing polymers meet the requirements of low toxicity and low smoke during combustion for environmental and health consideration [17,18]. The utilization of monomers containing phosphorus units, such as 9,10-dihydro-9-oxa-10-phosphaphenanthrene-10-oxide (**DOPO**), which possesses a polar P═O group and a bulky structure, resulted in polymers with good solubility. Moreover, incorporation of **DOPO** units into polymers also improved the adhesion and decreased the birefringence [19–27]. Aromatic polyesters containing **DOPO** pendent units have been prepared by the reaction of 2-(6-oxido-6H-dibenz<c,e><1,2>oxaphosphorin-6-yl)-1,4-benzenediol with different aromatic diacid chlorides in *o*-dichlorobenzene, at high temperature [28] or by the reaction of the same **DOPO**-containing diol with aromatic dicarboxylic acids using an $SOCl_2$/pyridine condensing agent [29].

Previously, we had prepared thermotropic polyesters and copolyesters from the polycondensation reactions of a diacid chloride, namely terephthaloyl-bis(4-oxybenzoyl-chloride), with 2-(6-oxido-6H-dibenz<c,e><1,2>oxaphosphorin-6-yl)-1,4-benzenediol, or with an equimolar amount of the latter and an aromatic or aliphatic diol [30,31]. The polymers had good thermal stability and some of them exhibited thermotropic behavior.

Here, we describe the results of the polycondensation of an aromatic bisphenol incorporating **DOPO**, 2-(6-oxido-6H-dibenz<c,e><1,2>oxaphosphorin-6-yl)-1,4-naphthalene diol **1**, or equimolecular amount of **1** and different diols **2**, with a diacid chloride containing two preformed ester groups **3**. The properties of the polymers such as solubility, thermal stability or glass transition temperature have been investigated. Mesogenic phases were

* Corresponding author. Tel.: +40 232 217454; fax: +40 232 211299.
E-mail address: tvladb@icmpp.ro (T. Vlad-Bubulac).

0032-3861/$ – see front matter © 2009 Elsevier Ltd. All rights reserved.
doi:10.1016/j.polymer.2009.03.017

observed with a hot-stage polarizing microscope. DSC and X-ray measurements were also performed.

2. Experimental

2.1. Synthesis of the monomers

2-(6-oxido-6H-dibenz<c,e><1,2>oxaphosphorin-6-yl)-1,4-naphthalene diol, **1**, was synthesized from **DOPO** and naphthoquinone [32]. It was recrystallised from ethoxyethanol; mp. (DSC): 279–280 °C. IR (KBr, cm^{-1}): 3430 (–OH), 1582 (P-Ph), 1190 (P═O), 1165 and 925 (P–O–Ph). ^1H NMR (DMSO-d_6, ppm): $\delta = 7.9$ (2H, m), 7.8 (1H, m), 7.7 (1H, m), 7.5 (4H, m), 7.4 (1H, m), 7.3 (1H, m). 7.2 (1H, t), 7.1 (1H, t), 6.6 (1H, d).

Terephthaloyl-bis-(4-oxybenzoyl-chloride), **3**, was synthesized by treating with excess thionyl chloride, at reflux temperature, of the corresponding dicarboxylic acid that resulted from the reaction of 4-hydroxybenzoic acid (2 mol) with terephthaloyl chloride (1 mol), according to a method presented in the literature [33]; mp.: 223–226 °C.

IR (KBr, cm^{-1}): 1780 (COCl), 1730 (COO), 1600 (aromatic), 1210 (Ph–O–OC).

The monomers **2**, such as ethylene glycol, 1,3-propanediol, 1,4-butanediol, 1,6-hexanediol and 1,12-dodecanediol, were provided from Aldrich and used as received.

2.2. Synthesis of the copolyesters *4*

A typical polycondensation was run as shown in the following example for the synthesis of polymer **4a**: In a 50 mL flask equipped with magnetic stirrer and nitrogen-inlet and outlet were introduced bisphenol **1** (1.329 g, 0.003 mol), diacid chloride **3** (1.044 g, 0.003 mol) and *o*-dichlorobenzene (7.5 mL). The reaction mixture was refluxed for 20 h, it was cooled to room temperature and poured into methanol (20 mL), under stirring, to obtain a precipitate which was filtered, washed with methanol, and dried at 100 °C for 10 h. For the synthesis of copolyesters **4b–4f** the same method was used, equimolecular amount of bisphenols **1** and **2** being added (Scheme 1).

Table 1
The inherent viscosities and elemental analysis of the polymers **4**.

Polymer	η_{inh} (dL/g)	Calculated (%)			Found (%)		
		C	H	P	C	H	P
4a	0.18	70.96	3.36	4.16	70.51	3.45	4.31
4b	0.21	69.39	3.49	2.64	68.92	3.67	2.91
4c	0.20	69.58	3.61	2.60	69.12	3.80	2.82
4d	0.22	69.77	3.74	2.57	69.42	3.94	2.73
4e	0.19	70.30	4.09	2.49	69.85	4.28	2.55
4f	0.23	71.28	4.74	2.32	71.01	4.90	2.47

2.3. Measurements

Melting points of the monomers and intermediates were measured on a Melt-Temp II (Laboratory Devices). Elemental analysis for phosphorus was performed with molybdenum blue method [34]. The inherent viscosities (η_{inh}) of the polymers were determined with an Ubbelohde viscometer, by using polymer solutions in chloroform: trifluoroacetic acid (9:1 v/v), at 20 °C, at a concentration of 0.5 g/dL.

Infrared spectra were recorded with a Specord M80 spectrometer by using KBr pellets. ^1H NMR spectra were recorded on a Bruker Avance DRX-400 spectrometer, using polymer solutions in deuterated chloroform: trifluoroacetic acid (9:1 v/v), at room temperature.

Thermogravimetric analysis (TGA) was performed in air at 10 °C/min with a Mettler Toledo model TGA/SDTA 851. The initial mass of the samples was 3–5 mg.

Differential scanning calorimetry (DSC) was performed with a Mettler TA Instrument DSC 12E at a heating rate of 10 °C/min under nitrogen atmosphere. The transition temperatures were read

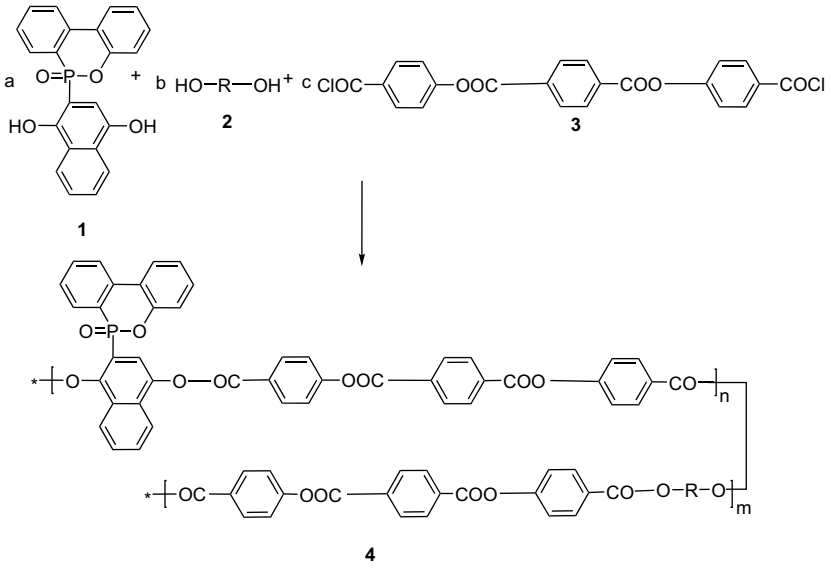

4a: a = 1 ; b = 0 ; c = 1 ; **4b**: a = 0,5 b = 0,5 c = 1 R = $(CH_2)_2$

4c: a = 0,5 b = 0,5 c = 1 R = $(CH_2)_3$ **4d**: a = 0,5 b = 0,5 c = 1 R = $(CH_2)_4$

4e: a = 0,5 b = 0,5 c = 1 R = $(CH_2)_6$ **4f**: a = 0,5 b = 0,5 c = 1 R = $(CH_2)_{12}$

Scheme 1. Preparation of copolyesters **4**.

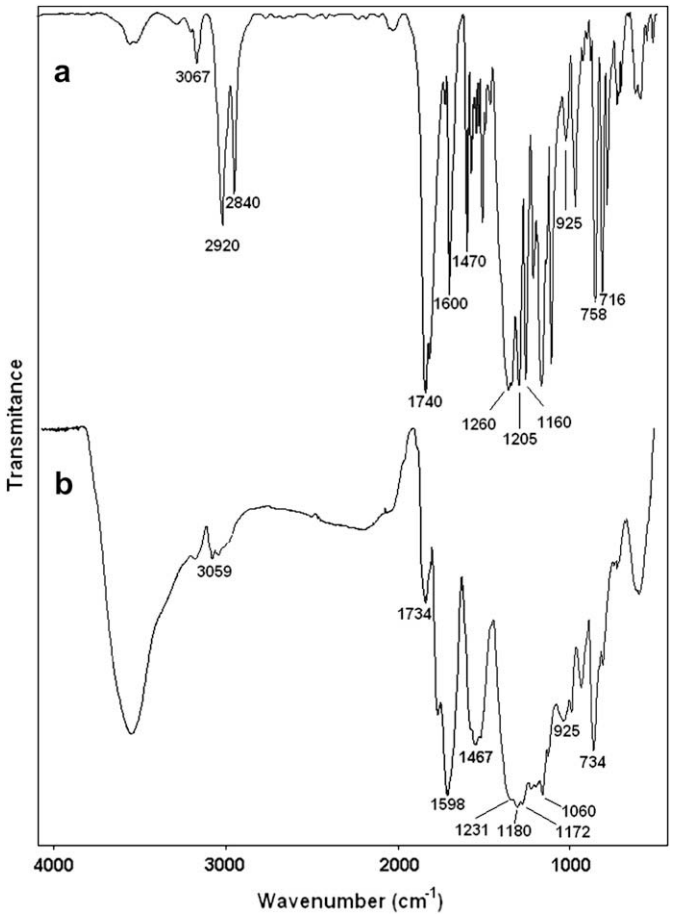

Fig. 1. IR spectra of polymer **4e** (a) unheated sample and (b) after heating up to 475 °C.

at the top of the endothermic and exothermic peaks. Heat flow vs. temperature scans from the second heating run was plotted and used for reporting the glass transition temperature. The mid-point of the inflexion curve resulting from the typical second heating was assigned as the glass transition temperature of the respective polymers.

Polarized light microscopy (POM) investigations were performed with an Olympus BH-2 polarized light microscope fitted with a THMS 600/HSF9I hot stage, at a magnification of 200× and 400×. The mesomorphic transition temperature and disappearance of birefringence, that is, the crystal-to-nematic (T_m) and nematic-to-isotropic (T_i) transition were noted.

Wide-angle X-ray diffraction (WAXD) measurements were performed using TUR-M62 diffractometer, and nickel-filtered Cu Kα radiation.

3. Results and discussion

3.1. Synthesis procedure and general characterization

Aromatic copolyesters **4** were synthesized from a **DOPO**-containing bisphenol **1** or an equimolecular amount of **1** and different diols **2** with a diacid chloride having two ester groups **3** (Scheme 1). The process was performed by heating the reaction mixture for 20 h at reflux temperature. The reaction system got temporarily homogeneous, than the polymers precipitated during the polycondensation process. The inherent viscosities of the polymers, measured in chloroform/trifluoroacetic acid (9:1 v/v) were in the range of 0.18–0.23 dL/g (Table 1).

The structure of the resulting polymers was investigated by elemental analysis, IR and ^{1}H NMR spectroscopy. The data obtained from elemental analysis for C, H and P content, showed that in all cases the determined carbon content was a little lower than the calculated one, probably due to the humidity absorption (Table 1). Fig. 1(a) shows the IR spectrum of polymer **4e**, as an example. The characteristic absorption peak at 1740 cm^{-1} was due to carbonyl asymmetric stretching of ester groups. The IR spectra showed also a broad weak absorption peak between 3600 cm^{-1} and 3200 cm^{-1} which is characteristic of the stretching vibration of unreacted OH groups. A longer reaction time did not lead to the disappearance of such weak absorption bands. Characteristic absorption peaks appeared at 925 cm^{-1} and 1160 cm^{-1} due to P–O–Ar groups, at 1470 cm^{-1} due to Ar–P groups and at 1205 cm^{-1} due to P═O

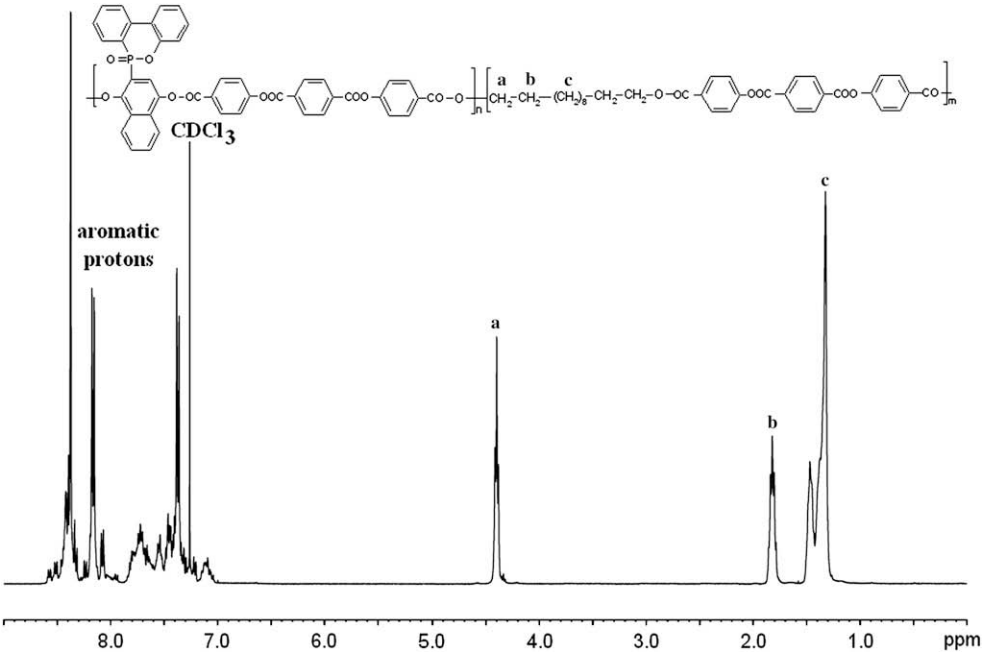

Fig. 2. ^{1}H NMR spectrum of the polymer **4f** in $CDCl_3$/trifluoroacetic acid, at room temperature.

groups. Aromatic C=C bands were found at 1600 cm^{-1} and 1500 cm^{-1}, while aromatic C–H absorption was found at 3070 cm^{-1}. In the case of the IR spectra of polymers **4b–4f** characteristic absorption bands appeared at 2920 cm^{-1} and 2830 cm^{-1} due to the presence of methylene groups.

The ^{1}H NMR spectrum of the polymer **4f** is presented in Fig. 2. As it can be seen the spectrum of the polymer **4f** exhibited characteristic peaks in the range of 8.54–7.09 ppm due to the presence of the aromatic protons and two broad singlets, which correspond to the methylene groups located in the α-position of the ester linkages (O–CH_2, 4H, peak a, Fig. 2) and in the β-position of the ester linkages, respectively (O–CH_2–$\underline{CH_2}$, 4H, peak b, Fig. 2). The peak characterizing the other methylene groups of the structural unit (CH_2, 16H, peak c, Fig. 2) appeared at about 1.37 ppm.

Except polymer **4f**, all other polymers were not soluble in organic solvents such as *N*-methyl-2-pyrrolidone or *N*,*N*-dimethylformamide but they were soluble in a mixture of chloroform/trifluoroacetic acid (9:1 v/v).

3.2. Mesophase identification

The morphological textures of the copolyesters were studied as a function of temperature in a hot-stage polarizing optical microscope. Photomicrographs of different textures are shown in Figs. 3 and 4. The data of the mesomorphic transition temperatures (K → LC and LC → I) are given in Table 2. All obtained polymers showed fine textures, difficult to ascribe, similar as reported for thermotropic polyesters based on terephthaloyl-bis(4-oxyphenylene carbonyl) units [12,16,35–37].

The transition temperature from crystal to liquid-crystalline melt was in the range of 205–259 °C and depends greatly on the content of aliphatic CH_2-groups. Melting transition temperatures decreased with increasing the number of methylene units. Thus, the copolyester **4f** based on 1,12-dodecanediol exhibited the lowest solid to LC mesophase transition (205 °C) while the polyester **4a** exhibited the highest value (259 °C). The isotropic phase for polymers **4b**, **4d** and **4e** was not detected up to initial thermal

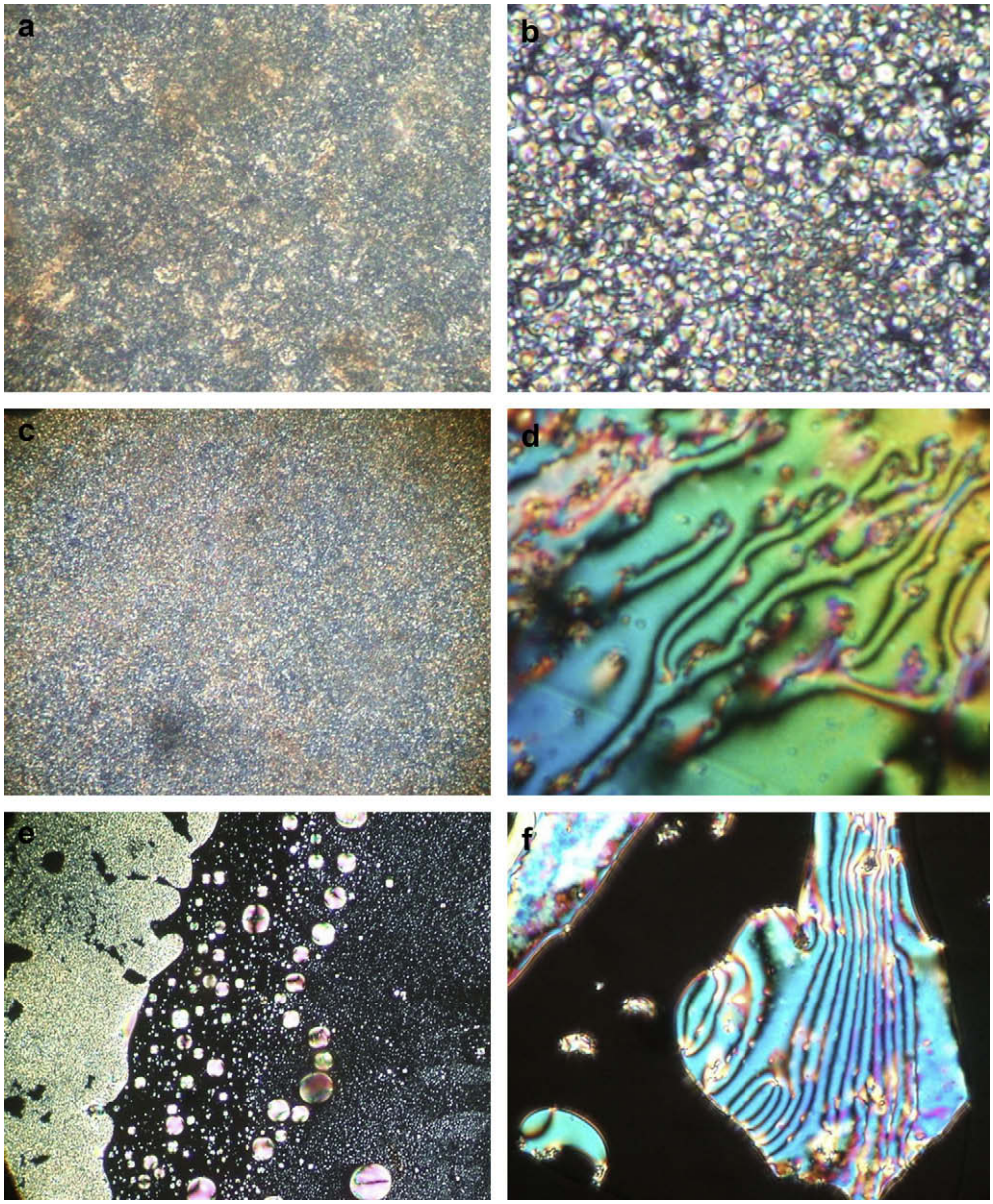

Fig. 3. Optical polarized micrographs for **4a** first heating at 270 °C (a) and second heating at 286 °C (b), **4b** first heating at 316 °C (c) and 390 °C (d), **4c** first heating at 334 °C (e) and 371 °C (f) (magnification 200×).

decomposition temperature. When the LC polymer melt sheared on glass plates, they exhibited a fine ordered nematic texture in the case of polyester **4a** (Fig. 3b), Schlieren nematic textures in the case of copolyesters **4b** and **4c** (Fig. 3d and 3f) or highly birefringence nematic textures in the case of copolyesters **4d** and **4e** (Fig. 4b and 4d). On cooling from isotropic state the polymers **4a**, **4c** and **4f** clearly revealed the appearance of a birefringence LC melt (Fig. 4f).

The transition temperatures of the copolyesters **4** measured by DSC were compared with those obtained from the optical polarized microscopy measurements. These two methods gave similar results which are listed in Table 2. The observed differences could be explained by the variation of heating/cooling rate, amounts of sample used and the presence of different atmosphere (nitrogen, in the case of DSC measurements and air, in the case of optical polarizing microscopy investigation).

The glass transition temperature (T_g), clearly seen in the second heating scan, was in the range of 96–146 °C (Table 2) being dependent on the nature of the aliphatic diols **2**. Thus, the fully aromatic polyester **4a** exhibited the highest T_g (146 °C). The introduction of an aliphatic diol decreased the T_g. It was observed that the T_g decreased by increasing the number of the methylene groups of the structure of the aliphatic diol. Polymer **4f** derived from 1,2-dodecanediol exhibited the lowest T_g (96 °C).

Thermal transitions for solution precipitated polymers were characterized by DSC measurements with a heating and cooling rate of 10 °C/min. Their phase transition temperatures of first heating scan and second heating scan are listed in Table 2. Typical DSC scanning curves for polymer **4f** are shown in Fig. 5. The DSC curves of polymers **4b**–**4f** showed multiple endotherms. This phenomenon of double melting was reported in many papers as a feature in common for liquid crystalline polyesters [38–40].

The DSC trace of the copolymer **4f**, obtained during the first scan, is illustrated in Fig. 5a. Upon heating from 20 °C to 350 °C the copolymer **4f** shows four different transitions: a double melting can

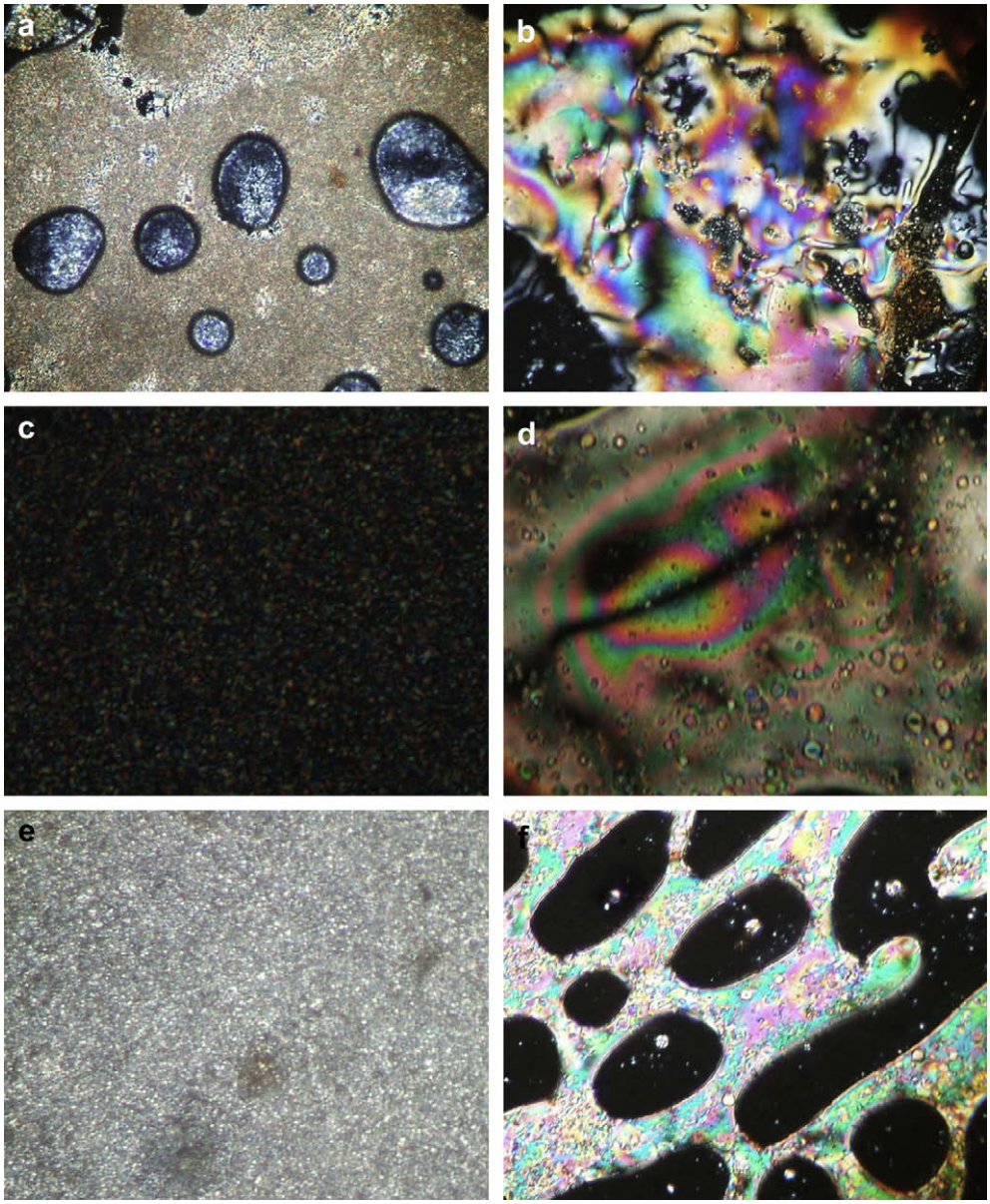

Fig. 4. Optical polarized micrographs for **4d** first heating at 270 °C (a) and 290 °C (b), **4e** first heating at 265 °C (c) and 307 °C (d), **4f** first heating at 216 °C (e) and first cooling at 247 °C (f) (magnification 200×).

Table 2
Phase transitions of the polymers **4** determined by DSC at scan rate of 10 °C/min on the first and second heating scans and microscopy observation.

Polymer	Thermal transition from DSC										Transition temperatures from POM (°C)
	First heating scan					Second heating scan					
	T_g (°C)	T_{m1} (°C)	T_{m2} (°C)	T (°C)	T_i (°C)	T_g (°C)	T_{m1} (°C)	T_{m2} (°C)	T (°C)	T_i (°C)	
4a	147	268	–	295	–	146	–	–	–	–	K259LC363I
4b	138	216	235	309	–	142	218	–	–	–	K254LC > 393I
4c	125	259	282	317	–	126	–	–	–	–	K250LC380I
4d	114	236	258	283	–	115	–	–	–	–	K250LC > 373I
4e	102	215	232	298	–	112	–	–	–	–	K241LC > 381I
4f	89	173	199	253	296	96	166	–	–	315	K205LC305I

T_g: Glass transition temperature; T_{m1}, T_{m2}: multiple melting transition; T: mesomorphic transition temperature; T_i: clearing point; K: crystal; LC: LC phase; I: isotropic phase.

be seen with endothermic peaks at 173 °C (T_{m1}) and 199 °C (T_{m2}) followed by one large endothermic peak centered at 253 °C and one tiny endothermic peak at 290 °C. The multiple melting behavior has previously attributed to reasons including the presence of different crystal structures [41,42] or to crystal reorganization [43,44] or to different components of the morphology formed in two stages of crystallization [45].

From a comparison with POM measurements we assigned the peaks at 173 °C and 199 °C to a crystal–LC transition and the peak at 290 °C to the corresponding nematic–isotropic transition. Second rescan of the polymer **4f** after cooling from the mesomorphic state (Fig. 5b) transformed the double melting peaks into one broad tiny endotherm (166 °C) while the T_i transition occurred at about 315 °C. The same behavior was observed for the copolyesters **4b**–**4e** with the exception that the T_i transition did not appear before 350 °C. The values for the T_{m1}, T_{m2} and T were listed in Table 2.

3.3. X-ray diffraction

The polymers **4** were subjected to wide-angle X-ray diffraction measurements, and the WXRD patterns are shown in Fig. 6. The % crystallinity, d-spacing values and Bragg angles of the copolyesters are summarized in Table 3. The polyester **4a** showed two main diffraction peaks at $2\theta = 16.4°$, $d = 5.4$ Å and $2\theta = 22.8°$, $d = 3.9$ Å, respectively, and some other small peaks (Fig. 6 – **4a**). Copolyesters **4b**–**4f** showed the two main diffraction peaks around $2\theta = 19.4°$ and $2\theta = 23.1°$ at different d values (Table 3). In the case of the copolyesters **4d**–**4f** the two main diffraction peaks appeared similar but more intense when compared with the copolyesters **4b** and **4c**. With the increasing content of methylene groups in every structural unit of copolyesters, the intensity of the original two main diffraction peaks for **4b** and **4c** increased and becomes sharper for the copolyesters **4d**–**4f**.

The % crystallinity of the polymers was determined by bisecting the experimental plot into crystalline domain and amorphous domain by curve fitting. The areas under the crystalline and amorphous domain are determined computationally and the % crystallinity was calculated. The % crystallinity varies from 11.7% to 26.2% depending upon their methylene groups content in the polymer. The % crystallinity initially decreases from 13.3%, in the case of polyester **4a**, to 11.7%, for the copolyester **4b** which contains two $-CH_2-$groups and increases by increasing the number of $-CH_2-$groups in the structural unit of the macromolecular chain. Thus, the copolymer **4f** based on 1,12-dodecanediol has the highest % crystallinity.

XRD pattern at different temperatures for the polymer **4f** is shown in Fig. 7. Temperature dependant X-ray diffraction diagrams at 24 °C, 190 °C, 220 °C and 240 °C, respectively, for the polymer **4f** were taken. At room temperature, the polymer **4f** possesses low-angle diffraction peaks at $2\theta = 3.83°$, $2\theta = 6.06°$ and $2\theta = 7.11°$ and four wide-angle peaks at $2\theta = 16.30°$, $2\theta = 19.25°$, $2\theta = 20.69°$ and $2\theta = 22.94°$ which suggest a layer ordered crystalline structure. Two diffraction peaks at $2\theta = 3.75°$ and $2\theta = 5.50°$ were visualized after heating the sample to mesomorphic state (190 °C) suggesting at this moment the presence of a smectic structure. The X-ray diffraction diagram at 240 °C shows only a broad reflection around

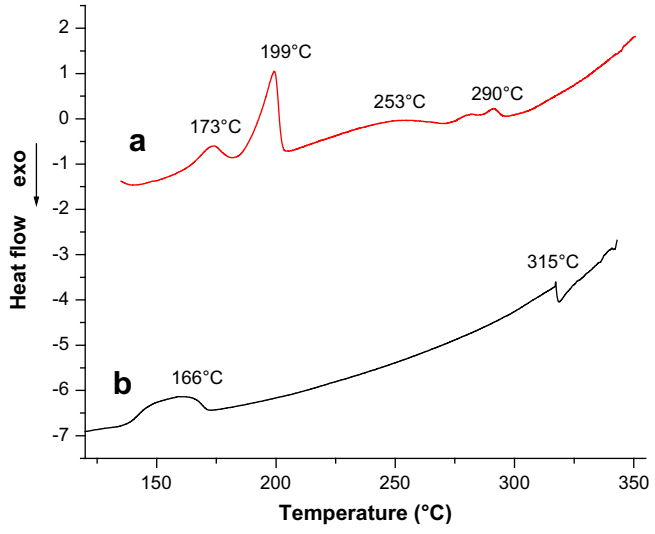

Fig. 5. DSC thermograms of the polymer **4f** for the first heating cycle (a) and the second heating cycle (b) at 10 °C/min.

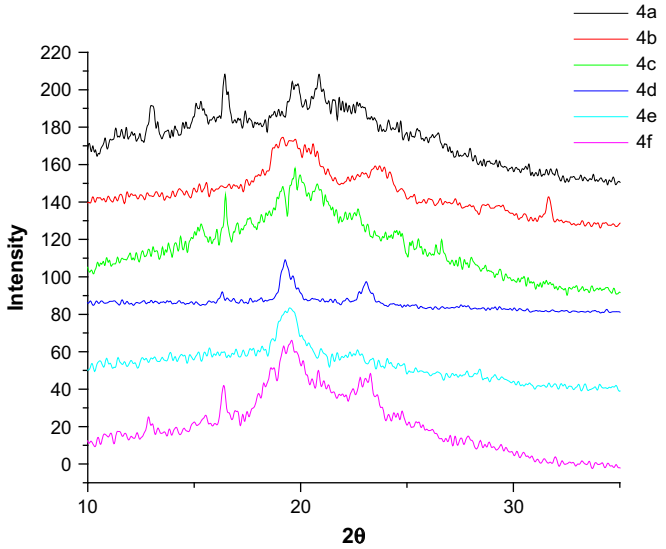

Fig. 6. Wide-angle X-ray diffractograms of the polymers **4**.

Table 3
Observed X-ray diffraction data for polyesters **4**.

Polymer	Peak (2θ) (°)	d-Spacing (Å)	Intensity	Crystallinity (%)
4a	16.4	5.4	sS	13.3
	17.5	5.1	vwB	
	19.8	4.5	sB	
	22.8	3.9	sS	
	23.5	3.8	mB	
4b	19.2	4.6	mB	11.7
	19.7	4.5	wB	
	23.6	3.8	mB	
4c	20.1	4.4	mB	12.8
	22.7	3.9	wB	
	24.5	3.6	wB	
4d	19.3	4.6	vsS	20.8
	23.1	3.9	sS	
4e	16.6	5.4	vwB	24.3
	19.4	4.6	vsS	
	23.1	3.9	wB	
4f	16.5	5.4	mS	26.2
	19.6	4.5	sS	
	21.1	4.2	mB	
	23.0	3.9	sB	

$2\theta = 19.66°$, the low-angle peaks disappeared indicating one less-ordered nematic mesophase.

3.4. Thermal stability

The thermo-oxidative stability was evaluated by thermogravimetric analysis (TGA) in air, at heating rate of 10 °C/min. Fig. 8 shows the TGA results generated on the **4a**, **4e** and **4f** samples under study. The most important TGA data (the initial decomposition temperature, temperature of DTG peaks, the yield of char residue at 600 °C) are also summarized in Table 4. The polymers did not show significant weight loss below 375 °C. They began to decompose in the range of 379–395 °C showing a 10% weight loss in the range of 385–407 °C.

As it can be seen from differential thermogravimetric (DTG) curves, the phosphorus-containing copolyesters decompose in a two-stage weight loss process. The first maximum of decomposition (T_{max1}) was in the range of 418–436 °C and was due to the destruction of ester units and **DOPO** groups which were more sensitive to degradation. The second maximum of the decomposition (T_{max2}) was in the range of 592–659 °C and was due to the degradation of polymer chain itself (Table 4). The FTIR spectrum of the solid residue of the polymer **4e**, after heating the sample up to 475 °C with the heating rate of 10 °C/min, was examined (Fig. 1b). The value of 475 °C represents the temperature of the end of the first decomposition process, from DTG curve (Fig. 8). As can be seen from Fig. 1 and as we discussed earlier, the most important absorption bands in the IR spectrum of unheated sample (spectrum a) are associated with aromatic C–H (3067 cm^{-1}, stretching vibration), aliphatic C–H (2920 cm^{-1} and 2840 cm^{-1}, asymmetric and symmetric stretching vibrations), C=O (1740 cm^{-1}, stretching vibration), ester C–O–C (1260 cm^{-1} and 1005 cm^{-1}, asymmetric and symmetric stretching vibrations), P–O (925 cm^{-1}, stretching vibration), aromatic C–H (758 cm^{-1}, deformation vibration caused by the 1,2-disubstituted aromatic **DOPO** rings), aromatic C–H (716 cm^{-1}, deformation vibration from aromatic terephthaloyl ring) [46,47].

Heating to 25% weight loss brings about a decrease in intensity of the aliphatic C–H, C=O and C–O–C ester absorption bands, associated with the decomposition of the ester bonds followed by the volatilization of the aliphatic moieties from the macromolecule. This process is almost complete at about 50% weight loss as the corresponding IR spectrum (Fig. 1b) does not exhibit the absorption bands characteristic for aliphatic structures. However, during the decomposition process, the C=O stretching vibration

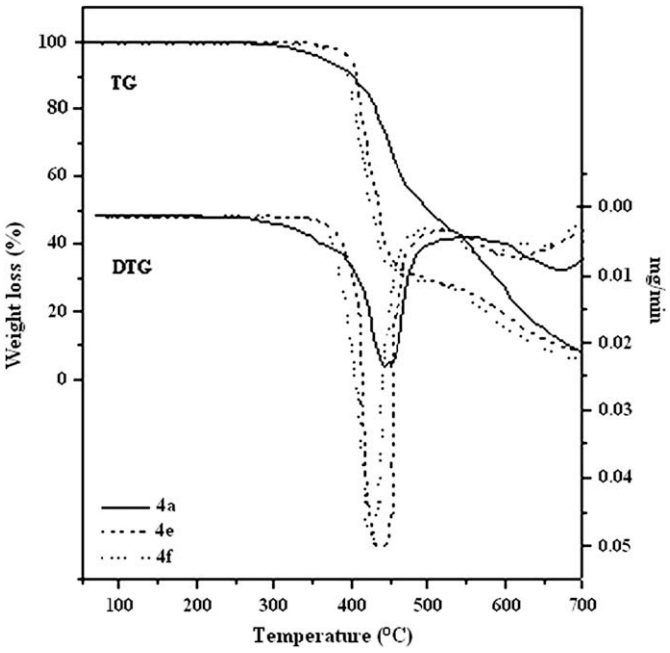

Fig. 8. TG and DTG curves of polymers **4a**, **4e** and **4f**.

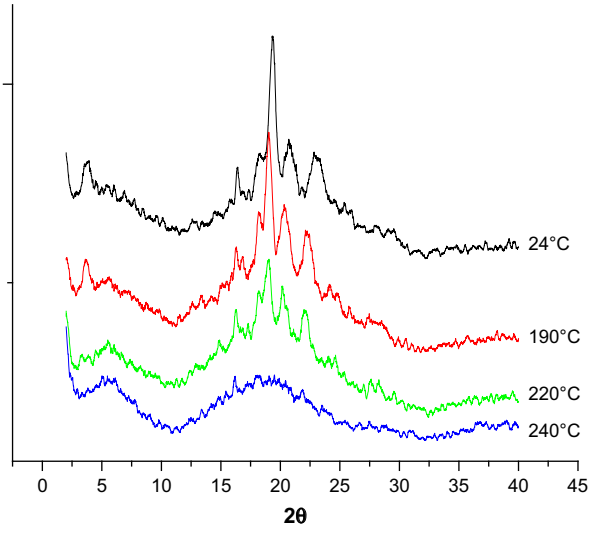

Fig. 7. XRD pattern of the polymer **4f** at different temperatures.

Table 4
Thermal properties of the polymers **4**.

Polymer	IDT[a] (°C)	T_{10}[b] (°C)	T_{max1}[c] (°C)	T_{max2}[d] (°C)	Char yield at 600 °C (%)
4a	385	403	436	659	28
4b	393	407	429	628	23
4c	381	388	419	625	22
4d	379	385	420	600	19.5
4e	395	405	418	603	17
4f	390	398	422	592	14

[a] Initial decomposition temperature = the temperature of 5% weight loss.
[b] Temperature of 10% weight loss.
[c] First maximum polymer decomposition temperature.
[d] Second maximum polymer decomposition temperature.

does not completely vanish, but becomes smaller and moves to 1734 cm^{-1}. The new position of the C═O stretching vibration is in agreement with that in polyarylates [46,48]. At this stage we may assume that a transformation of the aromatic–aliphatic copolyester to an aromatic–aromatic one may take place by disappearance, during the decomposition process, of the aliphatic moieties. The other new broad absorption bands located at 1231 cm^{-1}, 1172 cm^{-1}, 1060 cm^{-1} and 734 cm^{-1} are also in agreement with the formation of the aromatic–aromatic polyester. Another new broad absorption band centered at 1598 cm^{-1} is associated with the formation of polyaromatic structures [49]. The organophosphorus P–O–C group incorporated in the solid residue is distinguishable by the absorption band at 925 cm^{-1} [47]. The characteristic bands of P–C and P═O were observed at 1467 cm^{-1} and 1180 cm^{-1}, respectively indicating the presence of phosphorus in the solid residue. It can be concluded that in the first step of degradation, the destruction of aliphatic moieties and ester groups with an increase of phosphorus content took place. This agreed with the high char yield at high temperature. The char yields at 600 °C were in the range of 14–28% (Table 4). A decrease of char yield at 600 °C was observed by introduction of aliphatic diols with a higher number of methylene groups. The high char yield limits the production of combustible gases, decreases the exothermicity of the pyrolysis reactions of the polymers, inhibits the thermal conductivity of the burning materials, thus increasing the flame retardancy of the polyesters.

4. Conclusions

The polycondensation of 2-(6-oxido-6H-dibenz<c,e><1,2>oxaphosphorin-6-yl)-1,4-naphthalene diol **1**, or equimolecular amount of **1** and different aliphatic diols **2**, with terephthaloyl-bis-(4-oxybenzoyl-chloride), in *o*-dichlorobenzene, at high temperature, gave phosphorous-containing aromatic copolyesters. They exhibited good thermal stability, with decomposition temperature above 375 °C and glass transition temperatures in the range of 96–146 °C. The thermotropic liquid crystalline behavior occurred upon polymer melting was observed by POM and DSC. The phosphorous-containing copolyesters were shown by POM and X-ray diffraction to form liquid crystalline phases. The copolyester which had the lowest isotropization temperature was the polymer containing the longest flexible 12-methylene spacer linkage. LC copolyesters containing shorter 2,3,4 or 6-methylene flexible spacer units exhibited the most birefringent LC textures and, upon formation of the LC state, showed no isotropization temperature below 370 °C. The % crystallinity increases by increasing the number of $-CH_2-$ groups in the structural unit of the macromolecular chain.

Acknowledgements

The authors would like to thank Dr. Magda Aflori for X-ray analysis of the copolyesters.

References

[1] Economy J. J Macromol Sci Chem 1984;A21(13–14):1705–24.
[2] Bagheri M, Didehban K, Entezami AA. Eur Polym J 2005;41(3):611–7.
[3] Bhowmik PK, Han H, Cebe JJ, Burchett RA. J Polym Sci Part A Polym Chem 2002;40(1):141–55.
[4] He C, Lu Z, Zhao L, Chung TS. J Polym Sci Part A Polym Chem 2001;39(8):1242–8.
[5] Yerlikaya Z, Aksoy S, Bayramli E. J Polym Sci Part A Polym Chem 2001;39(19):3263–77.
[6] Sato M, Takeuchi S, Hino R. Macromol Rapid Commun 1999;20(7):373–7.
[7] Ranganathan T, Ramesh C, Kumar A. J Polym Sci Part A Polym Chem 2004;42(11):2734–46.
[8] Tejedor RM, Oriol L, Pinol M, Serrano JL, Strehmel V, Stiller B, et al. J Polym Sci Part A Polym Chem 2005;43(20):4907–21.
[9] Chen G, Lenz RW. J Polym Sci Polym Chem Ed 1984;22(11):3189–201.
[10] Acierno D, Fresa R, Iannelli P, Vacca P. Polymer 2000;41(11):4179–87.
[11] Desrosiers N, Bergeron JY, Belletete M, Durocher G, Leclerc M. Polymer 1996;37(4):675–80.
[12] Lin LL, Hong JL. Polymer 2000;41(12):4501–12.
[13] Cai R, Samulski ET. Macromolecules 1994;27(1):135–40.
[14] Bagheri M, Didehban K, Entezami AA. Iranian Polym J 2004;13:327–34.
[15] Lin LL, Hong JL. Polymer 2000;41(20):7471–81.
[16] Lin LL, Hong JL. Polymer 2001;42(3):1009–16.
[17] Liang H, Shi W. Polym Degrad Stab 2004;84(3):525–32.
[18] Petreus O, Popescu F, Barboiu V, Rosescu L. J Macromol Sci Chem 1988;A25(8):1033–8.
[19] Liu YL, Tsai SH. Polymer 2002;43(21):5757–62.
[20] Sun YM, Hung AYC, Wang CT. J Appl Polym Sci 2002;85(11):2367–76.
[21] Hoffmann T, Pospiech D, Haussler L, Komber H, Voigt D, Harnisch C, et al. Macromol Chem Phys 2005;206(4):423–31.
[22] Liou GS, Hsiao SH. J Polym Sci Part A Polym Chem 2002;40(4):459–70.
[23] Wang CS, Shieh JY, Sun YM. J Appl Polym Sci 1998;70(10):1959–64.
[24] Hamciuc C, Vlad-Bubulac T, Petreus O, Lisa G. Eur Polym J 2007;43(3):980–8.
[25] Vlad-Bubulac T, Hamciuc C, Petreus O, Bruma M. Polym Adv Technol 2006;17(9–10):647–52.
[26] Petreus O, Vlad-Bubulac T, Hamciuc C. Eur Polym J 2005;41(11):2663–70.
[27] Hamciuc C, Vlad-Bubulac T, Petreus O, Lisa G. Polym Bull 2008;60(5):657–64.
[28] Wang CS, Lin CH. Polymer 1999;40(15):4387–98.
[29] Vlad-Bubulac T, Hamciuc C, Petreus O. High Perform Polym 2006;18(3):255–64.
[30] Hamciuc C, Vlad-Bubulac T, Sava I, Petreus O. J Macromol Sci Part A Pure Appl Chem 2006;43(9):1355–64.
[31] Vlad-Bubulac T, Hamciuc C, Petreus O, Lisa G. Mater Plast (Bucharest) 2007;44(4):284–8.
[32] Sun YS, Wang CS. Polymer 2001;42(3):1035–45.
[33] Bilibin AY, Tenkovtsev AV, Piraner ON, Skorokhodov SS. Vysokomol Soedin 1984;A26(12):2570–6.
[34] Merz W. Microchim Acta 1959;47(3):456–65.
[35] McCarthy TF, Lenz RW, Kantor SW. Macromolecules 1997;30(10):2825–38.
[36] Ignatious F, Lenz RW, Kantor SW. Macromolecules 1994;27(19):5248–57.
[37] Skovby MHB, Lessel R, Kops J. J Polym Sci Part A Polym Chem 1990;28(1):75–87.
[38] Cheng SZD. Macromolecules 1988;21(8):2475–84.
[39] Li C, Xie X, Cao S. Polym Adv Technol 2002;13(3–4):178–87.
[40] Schneggenburger LA, Osenar P, Economy J. Macromolecules 1997;30(13):3754–8.
[41] Lovering EG, Wooden DC. J Polym Sci Polym Phys Ed 1969;7(10):1639–49.
[42] Samuel RJ. J Polym Sci Polym Phys Ed 1975;13(7):1417–46.
[43] Alfonso GC, Pedemonte E, Ponzetti L. Polymer 1979;20(1):104–12.
[44] Lee Y, Porter SR, Lin JS. Macromolecules 1989;22(4):1756–60.
[45] Basset DC, Olley RH, Al Raheil IAM. Polymer 1988;29(10):1745–54.
[46] Socrates G. Infrared and Raman characteristics groups frequencies: tables and charts. 3rd ed. Chichester: John Wiley & Sons; 2004.
[47] Thomas LC. Interpretation of the infrared spectra of organophosphorus compounds. London: Heyden; 1974.
[48] Balabanovich AI. J Anal Appl Pyrolysis 2004;72(2):229–33.
[49] Costa L, Avantaneo M, Bracco P, Brunella V. Polym Degrad Stab 2002;77(3):503–10.